AFCRL-69-0397

AD695121

AIR-LAUNCHED WINDSONDE

Stephen F. Rohrbough and Lyle E. Koehler
Honeywell Inc.
Systems and Research Division
Research Department
St. Paul, Minnesota 55113

Contract No. AF19(628)-6082
Project No. 6670
Task No. 667002
Work Unit No. 66700201
Scientific Report No. 1

July 1969

Contract Monitor: James F. Morrissey
Aerospace Instrumentation
Laboratory

Prepared for

AIR FORCE CAMBRIDGE RESEARCH LABORATORIES
OFFICE OF AEROSPACE RESEARCH
UNITED STATES AIR FORCE
BEDFORD, MASSACHUSETTS 01730

AFCRL-69-0397

AIR-LAUNCHED WINDSONDE

Stephen F. Rohrbough and Lyle E. Koehler
Honeywell Inc.
Systems and Research Division
Research Department
St. Paul, Minnesota 55113

Contract No. AF19(628)-6082
Project No. 6670
Task No. 667002
Work Unit No. 66700201
Scientific Report No. 1

July 1969

Contract Monitor: James F. Morrissey
Aerospace Instrumentation
Laboratory

Prepared for

AIR FORCE CAMBRIDGE RESEARCH LABORATORIES
OFFICE OF AEROSPACE RESEARCH
UNITED STATES AIR FORCE
BEDFORD, MASSACHUSETTS 01730

ABSTRACT

The design, development, and first phase of the testing of a wind measuring instrument are described. The device was required to obtain a vertical profile of winds to sea level after being released from an aircraft at 30,000 feet. An arrow shaped, low wind-drift sonde was selected that used an air-bearing gyroscope and magnetic field sensor to measure data that yielded wind shear. This information was then integrated to obtain wind velocity. The results of the balloon-launched phase of the field tests indicated that the sonde does respond to the wind and that the second test phase involving aircraft deployment of the sondes should be undertaken.

CONTENTS

ILLUSTRATIONS

TABLES

SECTION I
INTRODUCTION

A need exists to obtain vertical wind profiles over a large portion of the earth. To obtain these profiles it is essential that a sensor be developed that can be released from an aircraft and yield the information without requiring tracking of the sensor or loitering of the aircraft. Since the desired end result is to obtain a world-wide grid of vertical profiles, a large number of sensors will be required. This means that the ultimate cost of the individual sensor and sonde, in quantity, must be low. Thus, the following are guidelines in developing a system for obtaining wind profiles:

- Accurate wind measurement from 30,000 feet to sea level
- No tracking required
- High descent rate so that aircraft loitering is not required
- Inexpensive

A logical approach to the development of a wind sensing device required proof of feasibility of the sensing technique followed by field testing. The field testing can be broken into two phases. Since successful ejection from an aircraft is a difficult problem in itself, the first flight tests were scheduled as balloon drops. If these tests demonstrated system feasibility, the more difficult problem of aircraft ejection would be attempted. This report covers that period of the contract through the balloon flight tests.

SECTION II
TECHNICAL APPROACH

In the technical proposal (Ref. 1) leading to this program a number of approaches to wind measurement were presented. The most straightforward approach is to measure velocity directly. Alternately, one may measure acceleration and obtain velocity through integration, or measure position and obtain velocity through differentiation.

SENSING TECHNIQUES

A falling body can be designed to have any amount of wind drift. A system that determines the wind profile by measuring the accelerating forces acting on the body would be designed for small drift. On the other hand, a velocity or position measuring system would function more accurately with a large amount of wind drift, allowing the body to pick up the wind speed quickly. A small-wind-drift sonde generally requires a very high fall velocity. Since the sonde measures the resultant of the wind velocity and the fall velocity, a high fall rate requires that data be determined more accurately than for a sonde falling more slowly. However, the slow-falling sonde will wind drift more and have a longer fall time. Thus, it is more susceptible to time related errors.

Sonde Velocity Sensors

Investigations of various velocity measuring systems indicated that the most promising device would be a type of scanning doppler radar on a sonde that had a high wind drift. Even so, this approach had several objections. The first was the difficulty in getting good returns over a sea surface (and the effect of the water particle movement itself).

Next the effect of clouds below the sonde would complicate the measurement. Lastly, the individual cost in mass production appeared high.

Sonde Position Sensors

The possibility of accurately determining position of the sonde as it falls generally requires a tracking scheme (which violates the established guidelines) or a transponder system. The latter would yield position information to some known reference. In remote areas, this reference would have to be the deploying aircraft, and the accuracies required were beyond that of the aircraft position information.

Acceleration Sensors

Studies indicated acceleration measurement to be the best technique for gathering wind data. By using a fast-response arrow-shaped sonde design, accelerations could be inferred from attitude measurements. The sonde consists of the required electronic equipment placed in a non-lifting container rigidly connected by a tube to a lightweight lifting tail section. Such an aerodynamic body falling through the atmosphere will tilt away from vertical through an angle θ whose tangent is the relative wind (body drift velocity minus true wind speed) divided by the fall velocity. This angle then is related to the horizontal body acceleration, and thus, through an integration, the drift velocity can be determined. The axis of the sonde will lie in the wind direction plane and the angle ϕ of this plane from north gives the wind direction. The problems resolve into finding methods by which on-board measurements of the two angles could be made (see following sketch).

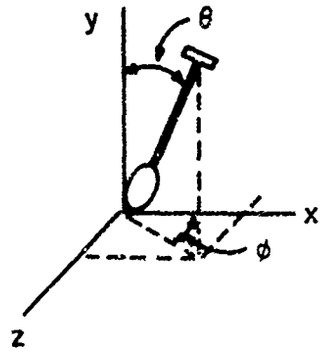

The solar-seeker method for attitude measurement was considered, but it has the obvious disadvantage of being usable only during daylight and when there are no interfering clouds. Other sun-related measurements that could eliminate the cloud interference problem generally have noisy signals.

The accelerations on the falling-arrow type sonde are along the axis of the sonde except during its response to a change in wind velocity. This means that there would be no information from the accelerometer during constant wind velocity conditions. Thus, the data could not be readily integrated to obtain the wind information. As a result spin-coils and the use of a gyroscope were examined to determine the vertical tilt angle. The results of this examination are presented in a subsequent discussion.

ARROWSONDE SIMULATIONS

To better understand the effects of fall rates and angle uncertainties, the mathematical relationships for the acceleration-type sonde were determined. A computer program that allowed changing of the various inputs was written to determine the effects of tilt angle error and ballistic parameter changes.

Tilt Angle Errors

It is possible to make good approximation of the total wind error when the uncertainty in θ takes the form of a constant error, using the simple formula derived here. The falling-arrow sonde responds rapidly to any change in relative wind velocity and aligns itself with the resultant wind V_R, as shown in the following sketch

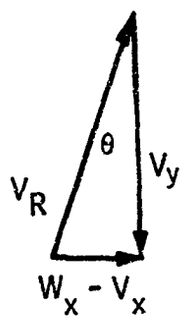

where the fall velocity is V_y, horizontal velocity of the sonde is V_x, and the horizontal wind velocity is W_x. The relative wind experienced by the sonde is $W_x - V_x$, and

$$W_x - V_x = V_y \tan \theta$$

When the arrow has fully weathercocked into this position, the resultant inertial acceleration is along a line joining the center of pressure and the center of mass, that is, along the sonde axis. The horizontal component may be denoted by a_x, and the vertical component is $g - \frac{dV_y}{dt}$.

Then $$a_x = \left(g - \frac{dV_y}{dt}\right) \tan \theta$$

The error in measuring the instantaneous relative wind, $W_x - V_x$, is related to the uncertainty in the measurement of θ by

$$\frac{\partial(W_x - V_x)}{\partial \theta} = V_y \sec^2 \theta$$

There is also an uncertainty in the drift velocity V_x after an elapsed time, t, because the acceleration in the x-direction is not precisely known. Here the dependence on the resolution in θ is

$$\frac{\partial V_x}{\partial \theta} = \frac{\partial}{\partial \theta} \int_o^t a_x dt = \int_o^t \left(g - \frac{dV_y}{dt}\right) \sec^2 \theta dt$$

Since θ is generally small (less than 5 degrees), $\sec^2 \theta$ is very nearly equal to one, and may be considered as a constant. With the further assumption of zero velocity at t = 0

$$\frac{\partial V_x}{\partial \theta} = \sec^2 \theta \int_o^t \left(g - \frac{dV_y}{dt}\right) dt = \sec^2 \theta \, (gt - V_y)$$

For the case under consideration, $\Delta\theta$ is a small fixed quantity. Then

$$\Delta(W_x - V_x) = V_y \sec^2 \theta \Delta\theta, \text{ and } \Delta V_x = (gt - V_y) \sec^2 \theta \Delta\theta$$

Summing these errors, the wind-measurement error is

$$\Delta W_x = gt \sec^2 \theta \Delta\theta \simeq gt \Delta\theta$$

Table I is a compilation of one of the computer simulation runs. The ballistic coefficient was taken to be 0.005 with a fixed bias error in θ of 0.5 degree. Included in the table are the altitude, fall time to reach that altitude, the wind velocity, W_x, the total error in W_x as measured by the sonde at that instant,

Table I. Error in Wind Magnitude for a Body with $\frac{C_D A}{W}$ = 0.005 and a Bias Error in θ of 0.5 degree

Altitude (1000 ft)	Fall Time (sec)	W_x (ft/sec)	Total Instantaneous Error in W_x (ft/sec)	Total Error in W_x Average over last 1000 feet (ft/sec)	θ (deg)	Total Calculated Instantaneous Error $\left[(t)(g)(\Delta\theta)(\sec^2\theta)\right]$ (ft/sec)
30	0	81.0	-	-	0	-
28	11.55	91.4	-3.25	-2.99	1.710	-3.24
26	16.60	122.6	-4.70	-4.47	4.506	-4.67
24	20.95	108.0	-5.91	-5.63	1.311	-5.88
21.9	24.95	50.0	-7.07	-6.81	-4.578*	-7.00
19.9	28.65	46.4	-8.11	-7.89	-4.032	-8.05
17.7	32.65	42.4	-9.23	-9.12	-3.555	-9.17
15.1	37.45	37.7	-10.58	-10.36	-3.111	-10.51
12.6	42.25	33.0	-11.93	-11.93	-2.761	-11.85
10.9	45.45	30.9	-12.83	-12.83	-2.566	-12.75
8.5	50.25	25.6	-14.18	-14.18	-2.319	-14.11
7.0	53.45	22.7	-15.08	-15.08	-2.179	-14.00
4.7	50.25	18.6	-16.43	-16.43	-1.999	-16.35
2.5	63.05	14.6	-17.77	-17.55	-1.849	-17.70
0.4	67.85	10.8	-19.12	-19.12	-1.724	-18.95

* In a two-dimensional wind profile the minus angle means that there has been a 180-degree shift in the wind direction.

the total error in W_x as measured by the sonde averaged over the preceding 1000 feet, and θ. Also included is the calculated total instantaneous error as determined from the expression derived above, $\Delta W_x = (t)(g)(\Delta\theta)(\sec^2\theta)$.

It is obvious from the table that, for such a sonde, a 0.5 degree uncorrected error in θ will result in approximately a 20ft/sec uncertainty at the end of the flight. If this θ error is reduced to 0.1 degree, the corresponding uncertainty in W_x at the end of the flight is 4 ft/sec. The above situation is a worst case; that is, the error has been considered as a fixed amount but unknown. In actual practice, $\Delta\theta$ is also a function of time. However, that portion of the error that is a fixed bias can be removed if a second "fix" on the actual wind is obtained at some later time in the flight.

Effect of Ballistic Parameter Change

To better understand the effect of different sonde fall rates on the required angle measurements, several computer simulation runs were made. A severe wind shear profile was established, and the value of the ballistic coefficient, $\frac{C_D A}{W}$, was changed for each run using the standard atmosphere density tables. This has the effect of changing the fall rate and fall time. From this, the wind drift effect at any moment can be analyzed with and without an error on the wind magnitude angle, θ. (For this analysis a two-dimensional wind profile was used.)

Several computer runs were made with ballistic coefficients ranging from 0.005 to 0.050. The former is a relatively low wind-drifting body while the latter has a rather large amount of wind drift. As expected, the larger ballistic coefficient allowed the arrow to weathercock to a larger angle; however, the higher wind drift meant that the angle quickly became small and was more difficult to determine.

In one of the computer simulation runs, the density profile was changed by 5 percent. This produced a maximum error in V_y of 2.5 percent. This also results in a 2.5 percent error in obtaining the relative wind $(W_x - V_x)$.

SECTION III
ARROWSONDE ATTITUDE MEASUREMENT

The Section II discussion states that the best approach was to make acceleration measurements on an arrow-shaped sonde having low wind-drift. Two methods were examined to determine the sonde orientation. The first was to use the magnetic-field vector measured by a spin-coil magnetometer plus the antenna-pattern null as seen by the aircraft. In the second a vertical reference gyro was employed for tilt angle and a magnetometer for wind direction.

SPIN-COIL TECHNIQUE

Initial effort expended on the spin-coil techniques was to determine the errors in the sonde tilt angle due to errors in the measurement of the spin coil voltage or phase and the antenna pattern (which determines the body roll position). The information from the spin coil generates the equation of a cone about the earth's magnetic field, the surface of which contains the sonde axis.

The original spin-coil arrowsonde concept had three mutually orthogonal coils; our analysis examined each coil separately, and the error equations in both the wind magnitude, θ, and direction, ϕ, were derived. The effect of various size errors in the maximum voltage measurement and the antenna position which is keyed to the coil were determined. The errors $d\theta$ and $d\phi$ are functions of ϕ, δ (the magnetic inclination), θ, and the measurement errors in coil voltage and antenna position.

Error Analysis of Z-Axis Coil

An error analysis was performed on part of the spin coil systems to determine the error model and restrictions for this sensing technique. Examined first was the Z-axis spin coil (rotating about the sonde axis) combined with a measurement of the angle with respect to the aircraft of a spinning antenna coupled mechanically to the spin coil. The information generated by the sonde is the phase angle between the spin-coil zero crossing and the antenna-pattern zero crossing (or marker) and the maximum voltage generated by the coil. Knowing the magnetic bearing of the aircraft and its altitude above the sonde, the magnetic field strength and inclination in the locality we can solve for the wind magnitude angle θ and the wind direction angle ϕ. The equations relating the above parameters are coupled, complex and require an iterative solution.

Figures 1 and 2 show the errors generated by a system using an error of 1 degree on the antenna pattern zero crossing (db) and a measurement error of one part in 1000 on the voltage maximum of the spin coil (de_{max}/e_{max}) added as

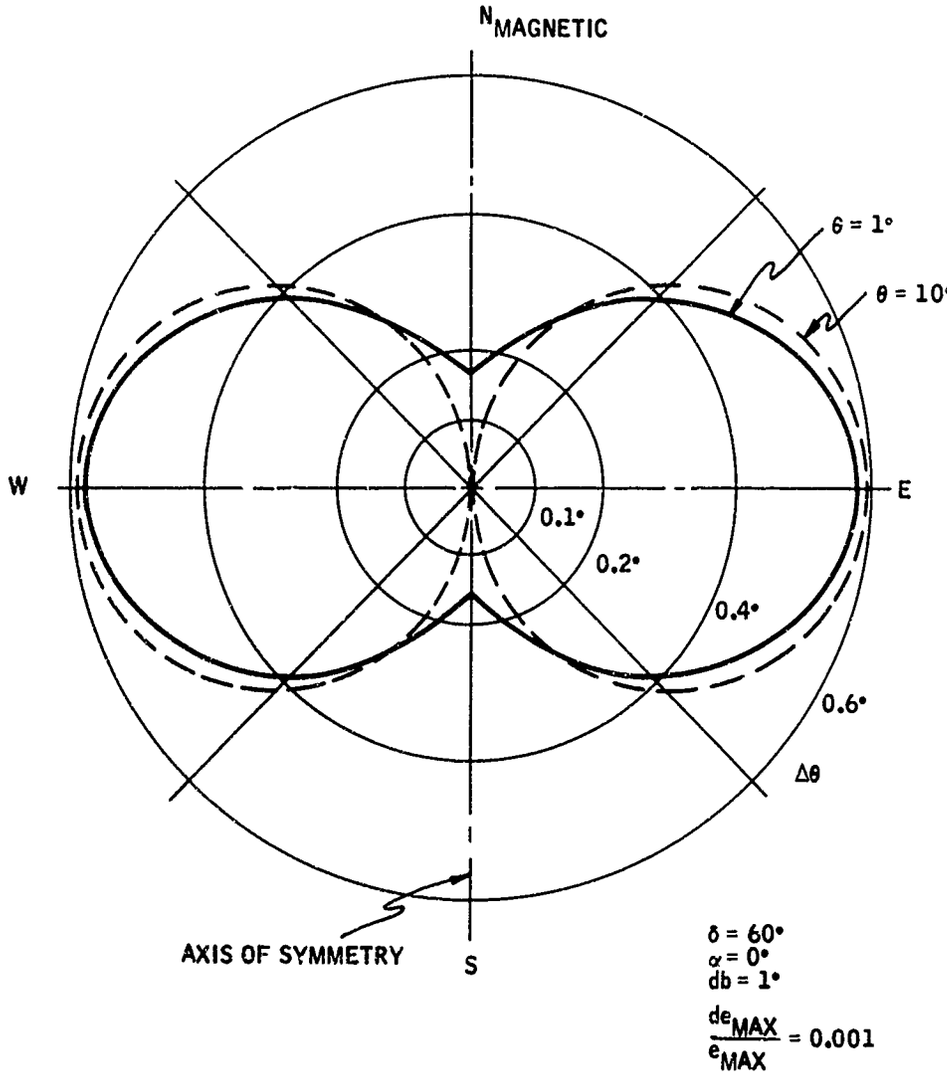

Figure 1. Wind Magnitude Errors Using Z' Axis Spin Coil and Antenna Pattern

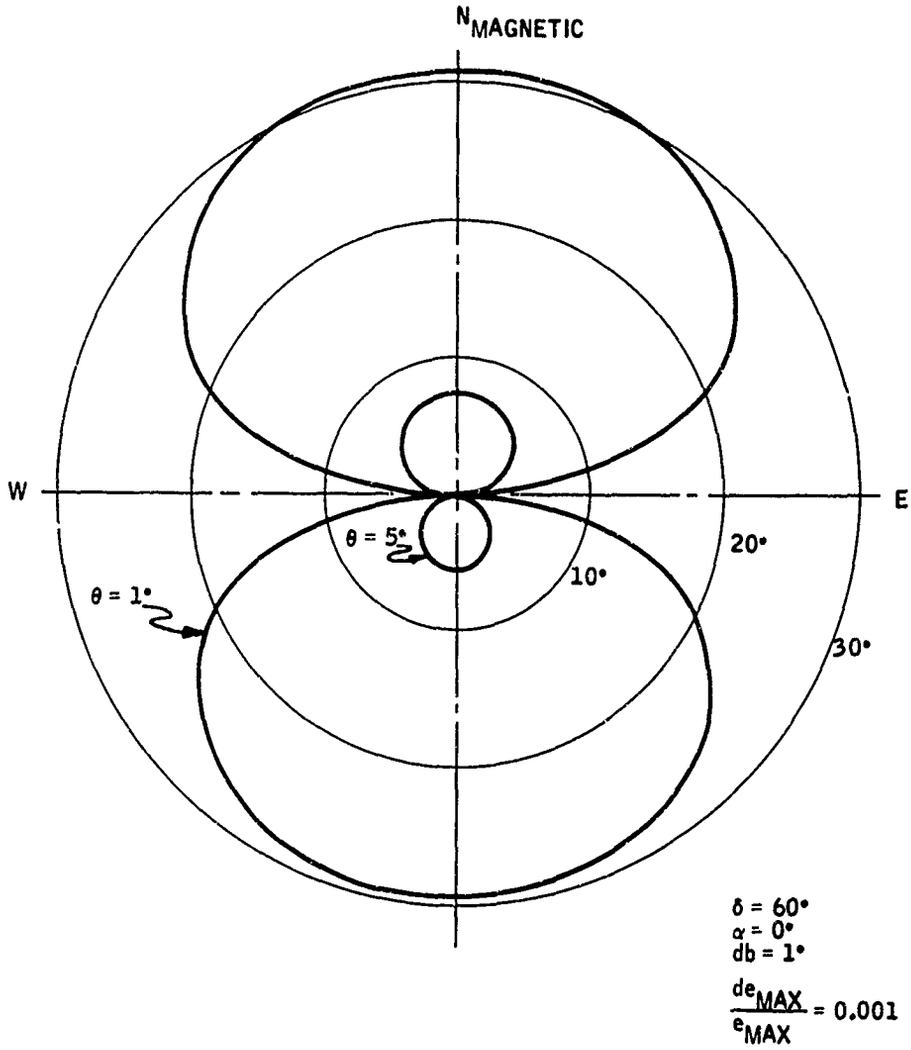

Figure 2. Wind Direction Errors Using Z' Axis Spin Coil and Antenna Pat'ern

RMS errors. In this instance the aircraft elevation is zero -- that is, the sonde is falling slowly such as would be the case for a shear probe and the aircraft is moving away rapidly so that the sonde tends always to be directly behind the aircraft, and the magnetic field inclination angle is 60 degrees. Note that for tilt angles (θ) of 1 degree and 10 degrees there is little difference in the tilt angle error for easterly or westerly winds, and the errors are a maximum of slightly more than one-half degree for these wind directions. If there were only north-south winds, then accuracies of close to 1/10 degree would be possible, and such accuracies would be entirely suitable even for true-wind measurements. At larger inclination angles (closer to the pole), accuracies will increase.

Also considered were aircraft elevation angles up to 45 degrees and aircraft bearing angles. The errors described above can be decreased by about 30 percent when the aircraft is flying a due south heading. The wind direction errors are a strong function of the tilt angle of the sonde. Note that the maximum wind direction error occurs 90 degrees away from the maximum error in the wind magnitude. For a tilt angle of 1 degree there is as much as a 30-degree uncertainty in the wind direction. However, very small tilt angles for slow-falling sondes mean very light winds, a case when the direction is not as important.

The errors plotted in Figures 1 and 2 are based on a full solution to the equation done on the computer.

With the assumption that the tilt angle is small, a relatively simple equation defining the errors can be established:

$$d\theta_{RMS} = \{ (\cot\delta\cos\phi)^2 db^2 + \left(\frac{de_{max}}{e_{max}}\right)^2 \left(\frac{180}{\pi}\right)^2 (\sin\theta - \cot\delta\sin\phi)^2 \}^{1/2} \text{degrees}$$

$$d\phi_{RMS} = \{ \left(1 - \frac{\sin\phi}{\tan\delta\sin\theta}\right)^2 db^2 + \left(\frac{de_{max}}{e_{max}}\right)^2 \left(\frac{180}{\pi}\right)^2 \left(\frac{\cos\phi}{\tan\delta\sin\theta}\right)^2 \}^{1/2} \text{degrees.}$$

These errors compare within a few percent to the full solution errors for all tilt angles of interest.

In the above discussion, the use of the radiating antenna pattern to assist in determining the wind information was suggested. An error of 1 degree in the antenna pattern was used in the error equations. The following discussion illustrates what accuracies are attainable theoretically, and what can be expected from an operational system.

We can, for example, postulate a transmitting antenna which has a pattern that results in a 100 percent sinusoidal modulation of the signal amplitude to a fixed receiver location when the transmitting antenna is rotated at a constant rate. Then the equation for angular resolution $\Delta\theta$ is

$$\Delta\theta = \frac{N}{V}\left(\frac{\pi}{\omega\ \tau_1}\right)^{1/2}$$

where N/V is the noise-to-signal voltage ratio, ω is the antenna rotation rate, and τ_1 is the sampling time. A numerical calculation based on this equation was presented in Reference 1 for the following conditions:

- Spin rate of 200 revolutions/second
- Transmitter power of 86 milliwatts
- Maximum range of 245 miles
- Sampling time of 2.5 seconds
- Receiving antenna effective aperture of 1 square foot
- Bandwidth of 1 kHz
- Effective antenna noise temperature of 300°K
- Transmitting antenna gain equal to 1/2 wave dipole

Angular resolution for these conditions is 5×10^{-3} radians, or about one-quarter degree. At closer range, the resolution for this ideal case would be better because the noise-to-signal ratio, and thus the angular uncertainty, varies linearly with range. Theoretically, then, resolution considerably better than one-quarter degree could be expected.

In practice, the transmitting antenna's pattern will almost certainly have some irregular, asymmetrical shape which varies with the relative elevation and polarization of the receiving antenna. Although a thorough experimental study would provide enough data on the pattern so the desired angle could be computed, there is no guarantee that antennas with identical radiation patterns could be mass-produced successfully. A further complication is that the signal path will not always be direct; i.e., reflections from the ground or from the airframe may completely alter the apparent orientation of the sonde. Ground reflections could lead to very large errors, while airframe reflections would introduce a secondary error related to polarization effects.

These difficulties are not insurmountable. By use of a pulsed transmission mode, the receiver could be gated to respond only to a direct signal. However, even with a sophisticated gating system, some interference may occur, and reflections from the airframe may not be eliminated. It is also possible to achieve high resolution by making the sonde's antenna extremely directional, but the dimensions would be prohibitive unless a frequency much higher than

1680 MHz is used. A very directional antenna also has the necessary disadvantage that the received signal amplitude fluctuates greatly during rotation such that, if the same transmitter is used for telemetry, the data quality may be seriously degraded.

There is one additional limitation. The relative bearing between sonde and aircraft also enters into the computation and may have an uncertainty considerably greater than one-quarter degree.

Errors Associated with X-Axis Coil

In addition, error equations for the X-axis spin coil, located perpendicular to the sonde axis, were derived. With such a coil, the sonde should be rotated about its axis to obtain the optimum (least error) position for solving the equations. These errors were comparable with those of the Z-axis coil.

Conclusions

From the foregoing discussion it is apparent that a precise analysis of the resolution attainable with a system meeting the cost limitations of an expendable sonde is very complex. However, the absolute orientation of the sonde may be determined with an accuracy approaching ±1 degree with moderate complexity; any substantial improvement on this figure would be costly.

GYROSCOPE TECHNIQUES

The second method of obtaining the vertical-tilt angle was through the use of a gyroscope. Such a sonde would use a free gyroscope to determine the angle between the sonde axis and local vertical. Thus, the wind magnitude would be read out directly, knowing the fall velocity, sonde drift velocity, etc., as before. The wind direction angle is obtained by having a magnetic field sensor keyed to the gyroscope. As the sonde rolls, the angle between magnetic north and the magnetometer (and thus the gyroscope reference) would be known. The combined outputs would then give the wind direction.

The selection of a gyroscope involved the establishment of a set of parameters that must be met. Since the sonde acquires a nearly horizontal position during ejection from an aircraft, the gyroscope must be constructed to allow a 90-degree maneuver with negligible drift. Since the roll position during ejection is uncertain, the gyroscope's rotor must have 360-degree freedom of motion in both axes. The only gyroscope that could meet these requirements was a gas-bearing free-rotor unit.

The Honeywell GG406 met the free-rotor requirement, but did not have the required drift accuracy over the mission time required for the windsonde because it was originally designed to run on missions of only 10 to 12 seconds.

However, replacement of the hollow rotor with a solid brass rotor increased the angular momentum and maintained a higher spin rate. With a solid-rotor unit, the major torques causing drift are: case rotation, autoerection, rotor unbalance, and bearing torque. For acceptable performance during the test program the drift rate had to be less than 0.5 deg/min. The modified GG406 had a predicted drift of 0.4 degree at the end of 1 minute and 1.2 degrees after 2 minutes. The mission time for the windsonde is anticipated to be less than 90 seconds.

Gyroscope Errors

A computer error analysis was made using selected values of gyroscope drift rates. Rates chosen varied from the best anticipated value of 0.1 deg/min to 0.5 deg/min. Eighteen runs were made using different wind profiles, drift-rate errors, and initial-condition errors. The results are presented in Figures 3, 4, and 5 and in Table II. The particular runs presented are for a high shear wind profile. However, there was no difference noted between the errors at any point for several other wind profiles considered.

The data were tabulated and plotted at approximately 2000-foot altitude intervals. The first four columns in Table II are, respectively, the sonde altitude, the time from launch to reach that altitude, the true wind speed (feet per second), and the tilt angle δ. Since only a two-dimensional wind profile was considered, the values for δ are both positive and negative. This means that a 180-degree change in the wind direction occurred. In the actual sonde, there will be no signs on the tilt angle; the wind direction will come from a second measurement.

The remaining four columns are each divided into three subcolumns: "a" is for a drift error of 0.1 degree after 1 minute (corresponds to Figure 3), "b" is for a drift error of 0.25 degree after 1 minute (corresponds to Figure 4), and "c" is for a drift error of 0.5 degree after 1 minute (corresponds to Figure 5). Column five is the error in feet per second in the calculated value of wind speed due only to the drift error in the gyroscope. Column six assumes that the true wind was unknown by 1.414 ft/sec at the time of the sonde release. This error and the wind error caused by the gyroscope drift, were then added at each data point as RMS errors. Column seven assumes that the accumulative alignment, uncaging, etc., errors add RMS and total 0.1414 degree. These were then added to the gyroscope-drift error at each data point as RMS errors before the wind error was calculated. Column eight then assumes both the errors in columns six and seven are present and essentially RMS adds column seven to six. Note that columns five, seven, and eight correspond to Cases 1, 2, and 3 in the figures, respectively. We also note that, under the worst conditions (Column seven and Figure 5, Case 3), the total error is less than 10 ft/sec down to an altitude of 9000 feet. With a 0.25-degree gyroscope-drift error, the error does not reach 10 ft/sec at any time. Other points can readily be obtained from the figures or table.

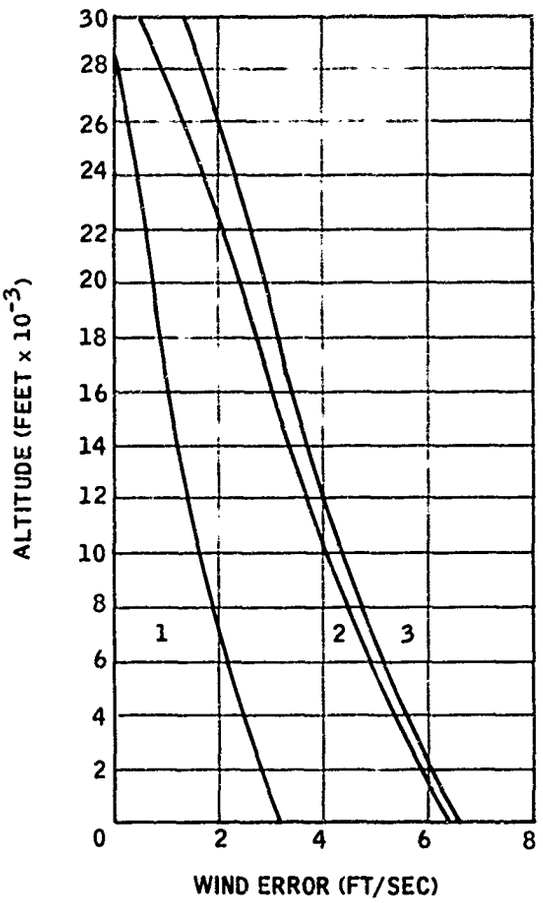

CASE 1. GYRO ERROR 0.1 DEGREE AFTER ONE MINUTE

CASE 2. GYRO ERROR 0.1 DEGREE AFTER ONE MINUTE RMS ADDED TO GYRO UNCERTAINTY OF 0.1414 DEGREE AT EACH POINT

CASE 3. ERROR OF CASE 2 RMS ADDED TO AN INITIAL CONDITION ERROR OF 1.414 FT/SEC

Figure 3. Wind Magnitude Error for 0.1 deg/min Gyroscope Drift

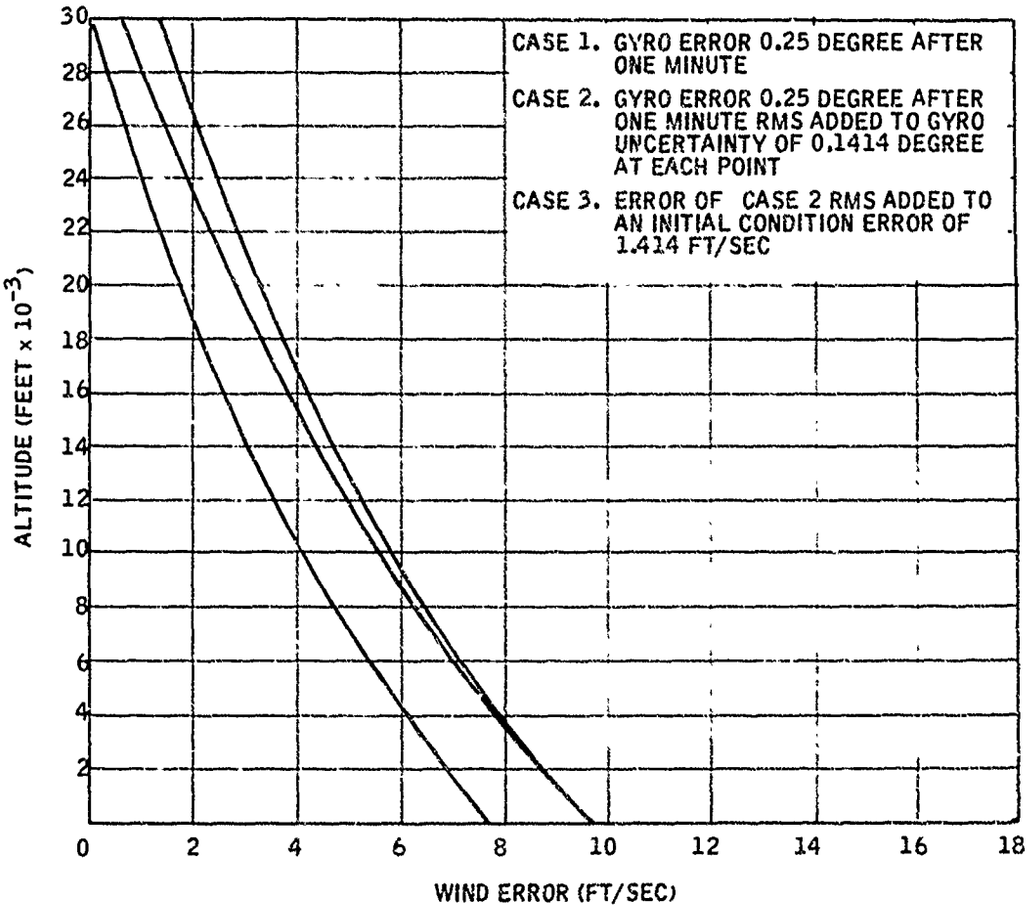

Figure 4. Wind Magnitude Error for 0.25 deg/min Gyroscope Drift

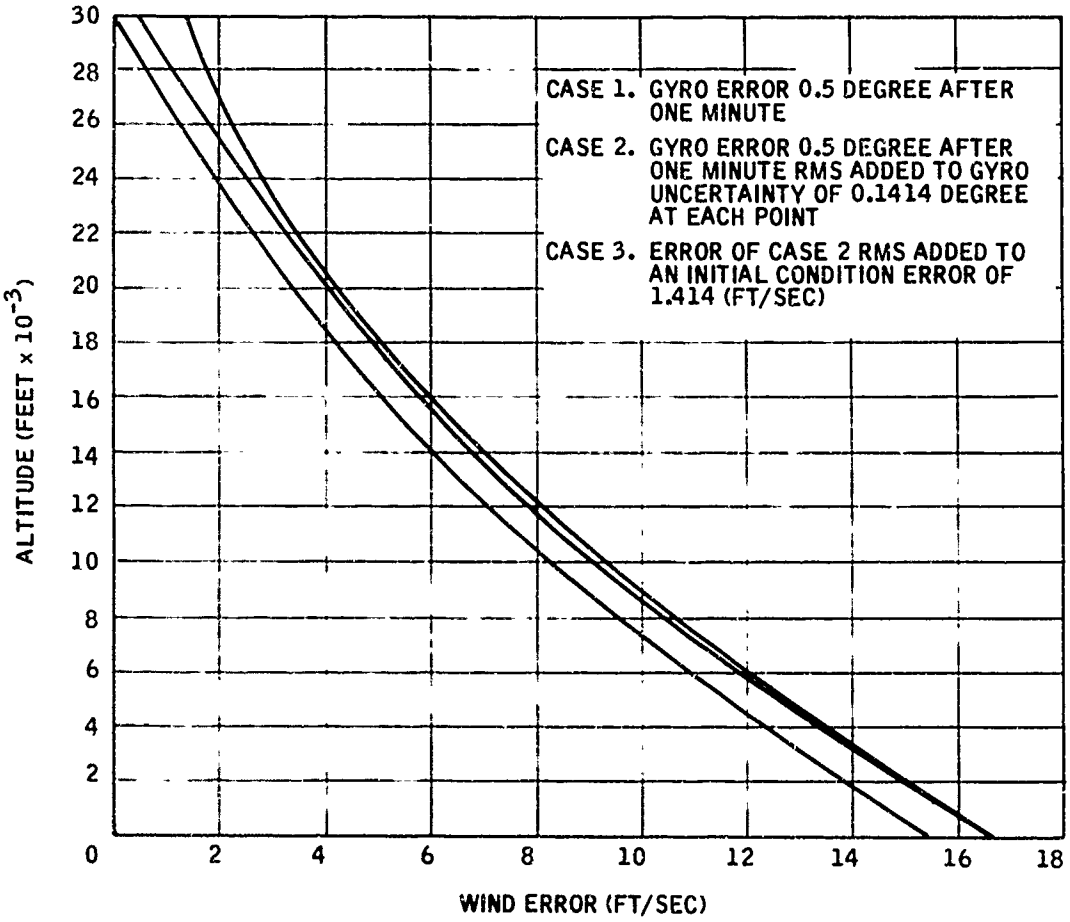

Figure 5. Wind Magnitude Error for 0.5 deg/min Gyroscope Drift

Table II. Wind Magnitude Errors Due to Gyroscope Drift and Initial Condition Errors

Altitude (1000 ft)	Fall Time (sec)	W_x (ft/sec)	θ (deg)	Error in W_x Due to Gyro-Drift Error (ft/sec)			Error in W_x Due to Gyro-Drift Error and Initial-Condition Error (ft/sec)			Error in W_x Due to Gyro-Drift Error and Gyro Uncertainty (ft/sec)			Error in W_x Due to Gyro-Drift Error, Uncertainty Error, and Initial-Condition Error (ft/sec)		
				a[a]	b[b]	c[c]	a	b	c	a	b	c	a	b	c
30.0	0	81.0	0	0	0	0	1.41	1.41	1.41	0	0	0	1.41	1.41	1.41
28.0	11.5	90.3	1.54	0.12	0.30	0.60	1.42	1.45	1.54	0.92	0.96	1.1	1.69	1.71	1.79
26.0	16.6	122.3	4.48	0.25	0.62	1.2	1.44	1.54	1.88	1.4	1.5	1.8	1.96	2.04	2.30
24.0	20.9	109.8	1.52	0.38	0.95	1.9	1.47	1.70	2.37	1.7	1.9	2.5	2.22	2.39	2.91
22.0	24.8	51.3	-4.50	0.53	1.3	2.6	1.51	1.93	2.99	2.1	2.4	3.3	2.50	2.78	3.61
19.9	28.8	46.3	-4.02	0.69	1.7	3.4	1.57	2.23	3.71	2.4	2.9	4.2	2.79	3.22	4.40
17.7	32.8	42.3	-3.54	0.87	2.2	4.3	1.66	2.59	4.55	2.8	3.4	5.1	3.11	3.71	5.29
15.5	36.8	38.3	-3.17	1.1	2.6	5.3	1.77	3.00	5.48	3.1	4.0	6.1	3.44	4.24	6.27
13.8	40.0	35.2	-2.92	1.2	3.1	6.1	1.87	3.37	6.28	3.4	4.5	7.0	3.71	4.69	7.11
11.7	44.0	31.4	-2.65	1.4	3.6	7.2	2.02	3.87	7.35	3.8	5.1	8.1	4.07	5.29	8.22
9.7	48.0	27.7	-2.43	1.7	4.2	8.4	2.19	4.42	8.49	4.2	5.8	9.3	4.44	5.92	9.40
7.3	52.8	23.3	-2.21	2.0	4.9	9.8	2.43	5.12	9.95	4.7	6.6	10.8	4.89	6.73	10.91
5.8	56.0	20.6	-2.08	2.2	5.4	10.9	2.60	5.62	11.0	5.0	7.2	11.9	5.21	7.29	11.96
3.6	60.8	16.5	-1.92	2.5	6.3	12.5	2.88	6.42	12.6	5.5	8.0	13.6	5.69	8.17	13.63
0.7	67.2	11.3	-1.74	3.0	7.4	14.8	3.29	7.56	14.9	6.2	9.3	15.9	6.36	9.42	16.00

a. $\Delta\theta$ = 0.10 degree after 1 minute

b. $\Delta\theta$ = 0.25 degree after 1 minute

c. $\Delta\theta$ = 0.50 degree after 1 minute

Prototype Testing

A modified version of the GG406 was built to determine if it would meet the desired specifications. For the prototype a 2-inch-diameter solid brass rotor was used. A hole drilled through the center of the sphere gave it a preferred spin axis and facilitated spinup. The gyroscope was assembled such that it could be spun up in two positions at right angles to one another. Optical pickoffs were used to eliminate the error imposed by the drag of the standard potentiometer pickoffs.

The spinup and uncaging of the gyroscope in the balloon-dropped windsondes was done by a motor with a teflon friction cone attached to its shaft. A mechanical linkage was used to withdraw the drive system and to uncage the gyroscope upon command.

Since the gyroscope's rotor might be spun up at right angles to the sonde axis, it was necessary to determine what error might occur in rotating the gyroscope body through 90 degrees as well as any uncaging error. A microscope was mounted to permit viewing of the top of the rotor. The magnification of the microscope allowed a 0.05-degree position change to be easily discernible. The rotor was then spun up and a null position determined with the motor attached. The motor was then withdrawn, and no detectable shift in the rotor position was noted. Repeated caging and uncaging actions showed no detectable shift in the spin axis due to the caging action.

During the 90-degree maneuver, the hole in the rotor must pass across a gas-bearing port. This applies a torque to the rotor. To determine the effect of this maneuver on the vertical alignment, a second test was made utilizing the microscope. With the gyroscope attached to a dividing head, the microscope was positioned to view the end of the rotor the same as it was during the uncaging tests. After spinup and uncaging, the gyroscope was rotated through 90 degrees and then back to its original position. No change in the spin-axis position was discernible. This process was repeated several times with the same results. The position of the microscope was then changed so that we could look at the rotor after the 90-degree maneuver. The rotor was spun up, the gyroscope rotated through 90 degrees, and a null position determined. The gyroscope was then returned to its original position, spun up, and rotated through 90 degrees. No change in the null position was noted. Repeated tests yielded the same results.

The outcome of these two tests indicate that the uncaging and 90-degree maneuver errors are nearly negligible, and they will certainly be less than the values used in the gyroscope error analysis presented earlier.

The run-down time constant (loss of 63 percent of the rotor's original speed) was about 2.2 minutes. Since the loss in angular momentum with speed matches the decrease in many of the error torques with speed, no significant deterioration in drift rate was noticed during long run-down times. The rotor spin

axis position was typically 1 degree at 1 minute, 10 degrees at 5 minutes and 15 degrees at 7 minutes from its starting position. The ball began to wobble due to loss of inertial stability and hydrostatic bearing torques at about 15 degrees and 8 minutes run-down.

Gyroscope Drift Measurement

The first measurements of the gyroscope drift were made with a rotor start speed of 12,000 rpm, and the average drift was approximately 2 deg/min. It appeared that most of the errors causing the drift were case oriented, and it was hypothesized that rotating the gyroscope case about the rotor's spin axis might average out these torques. A test was established that considered gyroscope case rotation comparable with those that would be acceptable for the falling windsonde. The gyroscope was mounted on a Genisco rate table and rotated at rates varying up to 3 rad/sec. With a rotation rate of at least 0.1 rad/sec, the drift rate decreased to around 0.2 deg/min for the first 2 minutes.

Details concerning the physical size, specifications, sources of drift, performance, and testing of the GG1003A can be found in 12042-QR4 (Ref. 2).

CHOICE OF GYROSCOPE TECHNIQUE

Based on the above discussion, it was apparent that the gyroscope vertical sensing technique best fit the established guidelines outlined earlier. It has sufficient accuracy and low enough drift when the sonde is rolling to yield accurate wind data. It does not require tracking of the sonde. Aircraft loitering is not required as the sonde will fall fast, and the gyroscope lends itself to mass production which is essential for an inexpensive sonde. As a result, the gyroscope was chosen as the vertical sensor.

SECTION IV
WINDSONDE DESIGN

With the sensing technique established, the design of the Windsonde itself was undertaken. The aerodynamic response of the sonde was established, and testing of prototype sondes completed before fabrication of sensing units was started.

AERODYNAMIC CONSIDERATIONS

The sonde forebody was required to be 4 inches in diameter due to the gyroscope's size. The error study implied that a fast-falling sonde was required, and a ballistic coefficient, $C_D A/W$, of 0.005 was chosen. With the drag coefficient of 0.5, the required total sonde weight is about 9 pounds. For ease of construction, the tail fin was made as a cruciform shape. A high aspect ratio is desired and low mass essential to achieve fast response and good damping of the sonde. Practical considerations led to the tail having a 6-inch span and a 2-inch chord. Then the lift coefficient is

$$k = \frac{a}{1 + \frac{2A}{b^2}} \approx 3.6$$

where A is the fin area, b is the span, and $a \approx 6$ per radian for this type fin.

To determine a reasonable length of the sonde, relationship between the moment of inertia and the damping coefficient was examined. From Reference 1 and rearranging terms, we find

$$\frac{4r^2}{\xi^2} = \frac{2I}{k \rho A r}$$

where r is the distance between the center of gravity and the center of pressure, ξ is the damping coefficient, I is the sonde's moment of inertia, k is the lift coefficient, ρ is the air density, and A is the fin area. As can be seen, r increases as the two-thirds power of ξ if all other terms remain equal. However, the moment of inertia will also increase with increasing r, making the total effect nearly one-to-one.

With r equal to 4 feet, (the largest value felt to be practical), the damping coefficient becomes approximately 0.45. While this is slightly more underdamped than desired, the response distance is quite small, indicating fast

response. From Figure 3-5 in Reference 1, a 50 percent response to a step change in wind with the above damping coefficient will occur in $0.2\lambda_n$.

$$\lambda_n = \frac{2\pi V_R}{\omega_n}$$

$$\omega_n = \frac{V_R}{\delta}$$

$$\delta = \frac{r}{2\xi}$$

so $\lambda_n = \frac{\pi r}{\xi} = 27.9$ feet

and $0.2\,\lambda_n = 5.6$ feet

Since other factors may affect the response of the sonde, it is safe to assume that a response distance of 8 to 10 feet will result.

WIND TUNNEL TESTS

A half-scale model of the proposed Windsonde was tested in a wind tunnel. Three forebody shapes were employed in the tests, each at two Mach numbers and three angles of attack. The center of pressure was cross plotted against Mach number for the 5- and 10-degree angle-of-attack tests. However, while the sonde body was held at a constant angle of attack, the tail section was flexed by the tunnel's dynamic pressure to a smaller angle. (During normal operating conditions, the entire sonde will respond when at an angle of attack.) As a result the true center of pressure will be better than that found in the tests.

Hemispherical, parabolic, and conical forebodies were tested, each at about Mach numbers of 0.3 and 0.5, and with 0, 5, and 10-degree angles of attack. With the exception of the 5-degree angle-of-attack parabolic forebody data, the drag coefficient for the sonde is 0.500 ± 0.090, within the limits of the tests. At high angles of attack, the cylindrical centerbody of the sonde has an effect on the measurements. This will produce a different drag force during the actual sonde flights, but it will act for only a short time due to the rapid response of the sonde. As a result of these tests, and the ease of fabrication of such a shape, the hemispherical shape was chosen for the Windsonde forebody. A complete description of the tests and their results may be found in Reference 2.

DUMMY SONDE TEST DROP

The tail boom on the half-scale model used during the wind tunnel tests was slightly shorter than 2 feet and appeared to vibrate during the tests. To minimize the moment of inertia of the sonde, it was necessary to hold the weight of the tail boom and fins to a minimum. Although the design provided a reasonable safety factor in the strength of these members, the possibility existed that a flutter mode might be set up in the cruciform fin and lead to mechanical failure. To determine whether the sonde had structural integrity, a dummy model of the sonde was constructed. A simple indicator of structural failure was provided in the test model by cementing very small wires to the edges of the fins and connecting these wires in series with the battery supply for a 27-MHz beacon transmitter.

Another important design feature which required an experimental check was the sonde's roll rate. To provide this information, a blocking oscillator modulated the transmitter at a frequency which was determined by the resistance of a photoconductive cell. In addition to the electronics, the sonde contained sufficient ballast to bring its weight up to the design value. Recovery of the test sonde was desirable, even though it was totally destroyed, because the distribution of parts would provide back-up information on whether failure occurred during flight. There was a possibility that the sonde would be tracked visually during its fall, so the sonde was painted dull black on one side, leaving the other half bright aluminum.

The dummy sonde was dropped from an altitude of 11,000 feet over Camp McCoy, Wisconsin. During the drop, the sonde was observed from the aircraft for the first portion of its flight, but visual contact was not made by the observers on the ground. However, the beacon transmitter functioned throughout the flight, indicating that the tail assembly remained intact. Fall time was 29 seconds, as predicted, so the actual drag coefficient of the sonde was very close to the calculated value.

The roll-rate signal was distinct for a little more than half the flight until the hazy sky conditions masked the roll signal. The roll rate was approximately 1.5 revolutions per second throughout the flight. It is interesting that the sonde's angular velocity varied so little as its airspeed increased from 120 ft/sec at release to approximately 400 ft/sec in mid-flight. With canted tail fins to induce roll, the equilibrium angular velocity should be proportional to airspeed. In this test, however, the sonde continued to roll at the rate imparted to it as it left the launch fixture. This rate was very close to the 1-rps terminal roll rate designed into the tail fins. Examining the torques and moment of inertia involved, we found that many seconds are required for the sonde to approach its equilibrium roll rate when its airspeed is low. If the sonde is dropped with no initial rotation, it will therefore take much longer to acquire a satisfactory roll rate than an estimate which assumes a linear variation with airspeed would indicate.

An adequate roll rate is essential not only to obtain roll position information from the aspect sensor, but also to minimize gyro drift. Accurate wind measurements thus require that the sonde be given an initial rotation.

ELECTRONICS DESIGN

With the mechanical strength of the sonde established, the electronics were investigated. The sonde's electronics were required to handle the gyroscope's pickoff outputs and direction information signal, the then transmit this data to a suitable ground receiving station. The ground station receives, processes, and stores the information for later data analysis.

Sonde Electronics

The gyroscope yields the tilt angle of the sonde from vertical, but another sensor is required to establish the angular orientation of the sonde about its roll axis. Sensors to detect the sun's position and the earth's magnetic field were considered. A photoconductor to detect the sun's position is not desirable since this requires daylight and clear sky conditions. As a result some form of magnetometer was considered. Either a Hall-effect device or a fluxgate magnetometer would meet the size requirements of the Windsonde, but it is unlikely that a fluxgate magnetometer could be produced at low enough cost for use in an expendable sonde. Although Hall-effect devices would probably serve the purpose, they have the disadvantage of low sensitivity. To produce a usable output signal in the earth's field, flux concentrators, a fairly high primary current, and further signal amplification would be necessary to raise the signal level high enough to modulate the telemetry transmitter.

A data transmission technique was chosen which calls for a subcarrier signal to be modulated by one of the gyroscope pickoff signals. The subcarrier generator can be directly modulated by the earth's magnetic field as well. Since the permeability of ferromagnetic materials is a function of the applied magnetic field, the inductance of an iron-core coil can be influenced by an external field. This holds true for powdered-iron cores used in many radio-frequency applications. Generally, such materials are selected to have a constant permeability in weak fields, but as saturation is approached there is a region in which permeability changes rapidly with applied field. Thus an oscillator using an iron-core coil which is biased by a strong magnetic field will have an operating frequency that is quite sensitive to field changes.

A breadboard model of this magnetometer subcarrier generator was constructed, using a slight variation of the basic scheme. Two oscillators operating in the 1-MHz range were adjusted to give a difference frequency of approximately 100 kHz. The oscillator coils had powdered-iron cores biased in opposite directions by small permanent magnets. Mixing the two signals produced a 100-kHz subcarrier which was subsequently amplitude-

modulated by one of the pickoff signals. Advantages of the difference-frequency technique are high sensitivity and good stability, since such factors as temperature drift are cancelled, while magnetic effects are doubled.

Figure 6 is a schematic diagram of the electronics for the first balloon-dropped sondes. In addition to the oscillator-mixer circuit described above, there is an integrated-circuit linear amplifier which brings the signal from pickoff 2 to a level which is sufficient to modulate the 135-kHz subcarrier and an emitter-follower circuit which provides impedance matching from pickoff 1 to a summing circuit. In the summing circuit, the modulated subcarrier and pickoff 1 signals are added linearly; the composite waveform is then applied to the frequency-modulation terminals of the 1680-MHz transmitter.

Ground Station Electronics

The ground station for the balloon tests operated in the following manner: From the antenna, the 1680-MHz signal was fed to the mixer or parametric down-converter, emerging at the 30-MHz intermediate frequency. At this point it was fed both to the GMD receiver and to a Nems-Clarke 1037 receiver. At the output of the Nems-Clarke's wideband FM detector, low-pass and high-pass filters separated the pickoff 1 signal from the modulated subcarrier. The pickoff 1 signal could be fed directly to the recorder. When the modulated subcarrier was fed to the FM and AM detectors, the magnetometer and pickoff 2 signals, respectively, were recovered and fed to the recorder to be stored on magnetic tape for later computation.

Additional details of the airborne and ground station electronics can be found in Quarterly Reports 4 through 6 (Refs 2, 3, and 4).

Sonde Release System

Three sondes were to be dropped for the first balloon flight test. The second flight test had two sets of four sondes. As a result the sonde cutdown control circuit was built to handle four units. A schematic of the circuit can be seen in Figure 7. The circuit was designed to reduce any interference between sondes as well as to protect each sonde from possible short circuits that might occur during a sonde's release.

The first ground command signal advanced the stepping switch one-half step and sent an unlatch signal to each sonde, ensuring that the power was off in each sonde. The second command signal advanced the stepping switch one-half step, removed the unlatch command, and began the start up sequence of the first sonde. A latching relay turned on the -18 volts and -12 volts in the sonde, activating the transmitter. A 55-second thermal delay relay was also activated. At the end of the delay, the piston actuator on the gas supply was fired, giving support to the gyroscope. The spinup motor was also started at this time. Had the piston actuator leads shorted upon firing, the fuse Fu5-1

would have opened, protecting the spinup circuit. Thirty-five to forty seconds were required to spin up the gyroscope.

Gyroscope uncaging and sonde cutdown were initiated by a third ground command. This first actuated EC2-1, a smokeless squib that uncaged the gyroscope. After a 1-second delay, the cutdown squib EC 1-1 was actuated. This cut the supporting cords and the six electrical leads going to the sonde. During this 1-second delay, the gyroscope was uncaged while the sonde was hanging vertical, providing the vertical reference. If any of the cut wires shorted to one another or to ground, operation of other sondes was unaffected since each line was fused to protect the power supply and cutdown circuit. The remaining sondes were released by repeating the same sequence of commands.

GYROSCOPE GAS BOTTLE TEST

The gas supply for the gyroscope was contained in a steel bottle 3 inches in diameter with a 0.050-inch-thick wall. Since the bottle was filled to 4000 psi, there was some concern about what would happen to the bottle if it were to break. Because of this concern a test was established that would subject a filled bottle to high stresses. A bottle that had been filled and armed was dropped from a height of 6 feet and then from 40 feet onto a concrete slab. Examination of the bottle after the drops indicated that it and its piston actuator were intact. The actuator was fired, the bottle top opened, and the gas flow timed showing that the drop had not affected its operation nor endangered anyone.

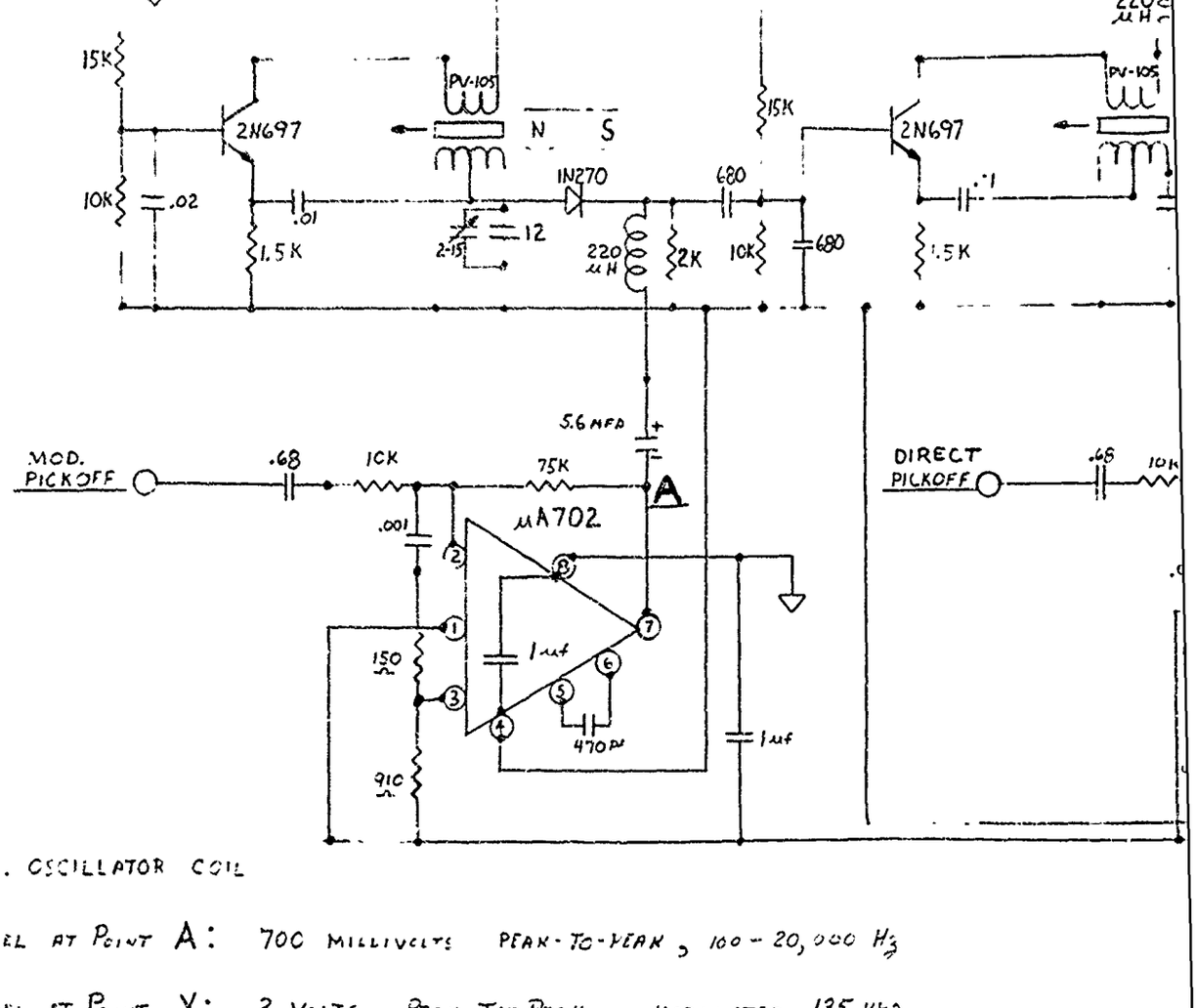

PV-105: B.C. OSCILLATOR COIL

SIGNAL LEVEL AT POINT A: 700 MILLIVOLTS PEAK-TO-PEAK, 100 - 20,000 Hz

SIGNAL LEVEL AT POINT X: 3 VOLTS PEAK-TO-PEAK, MODULATED 135 KHz

APPROXIMATELY 50% MODULATION (CARRIER LEVEL = 2 VOLTS PEAK-TO-PEAK)

Figure 6. Schematic Diagram of Sonde Elect

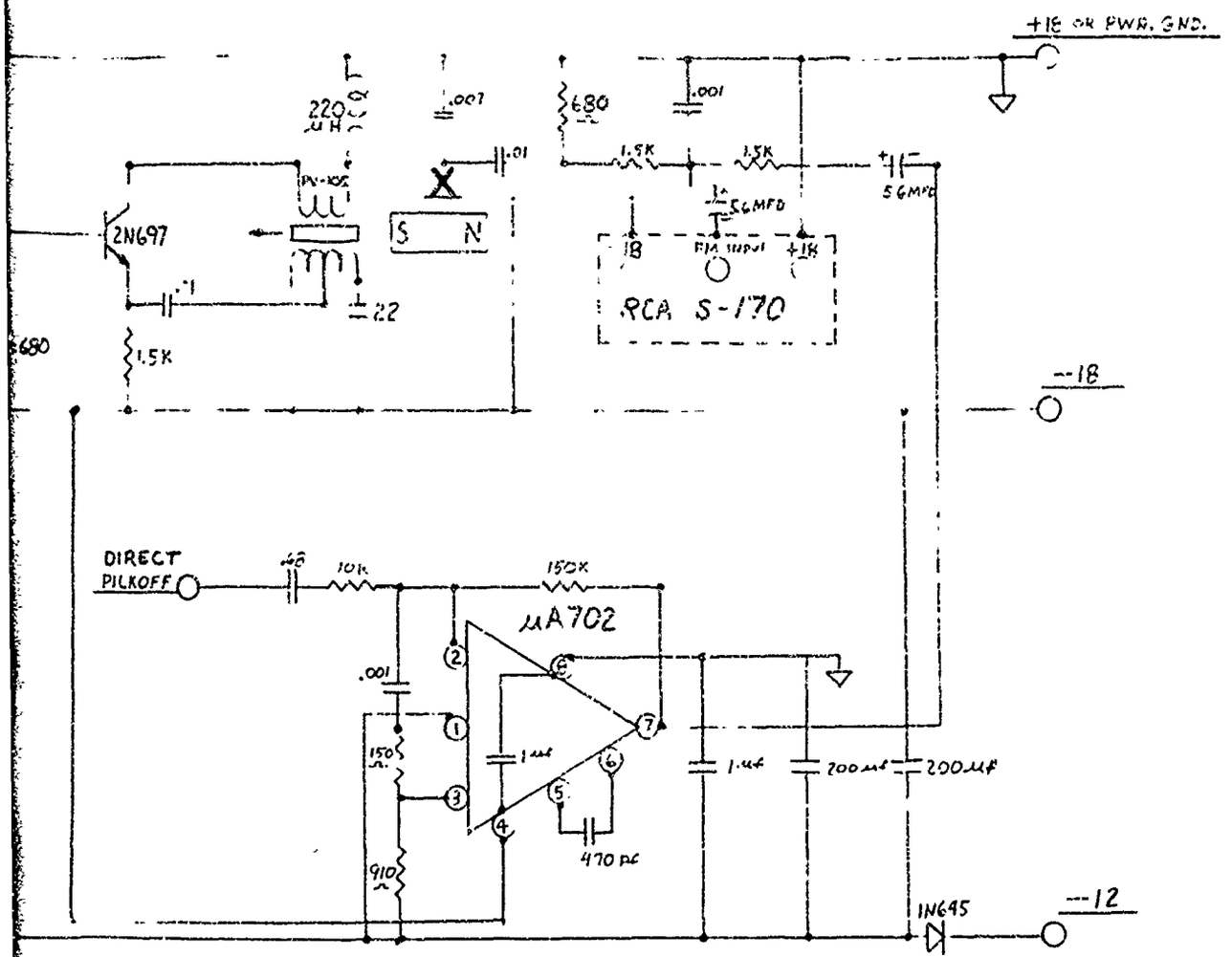

oo H_3

35 KH3

o-PEAK)

c Diagram of Sonde Electronics

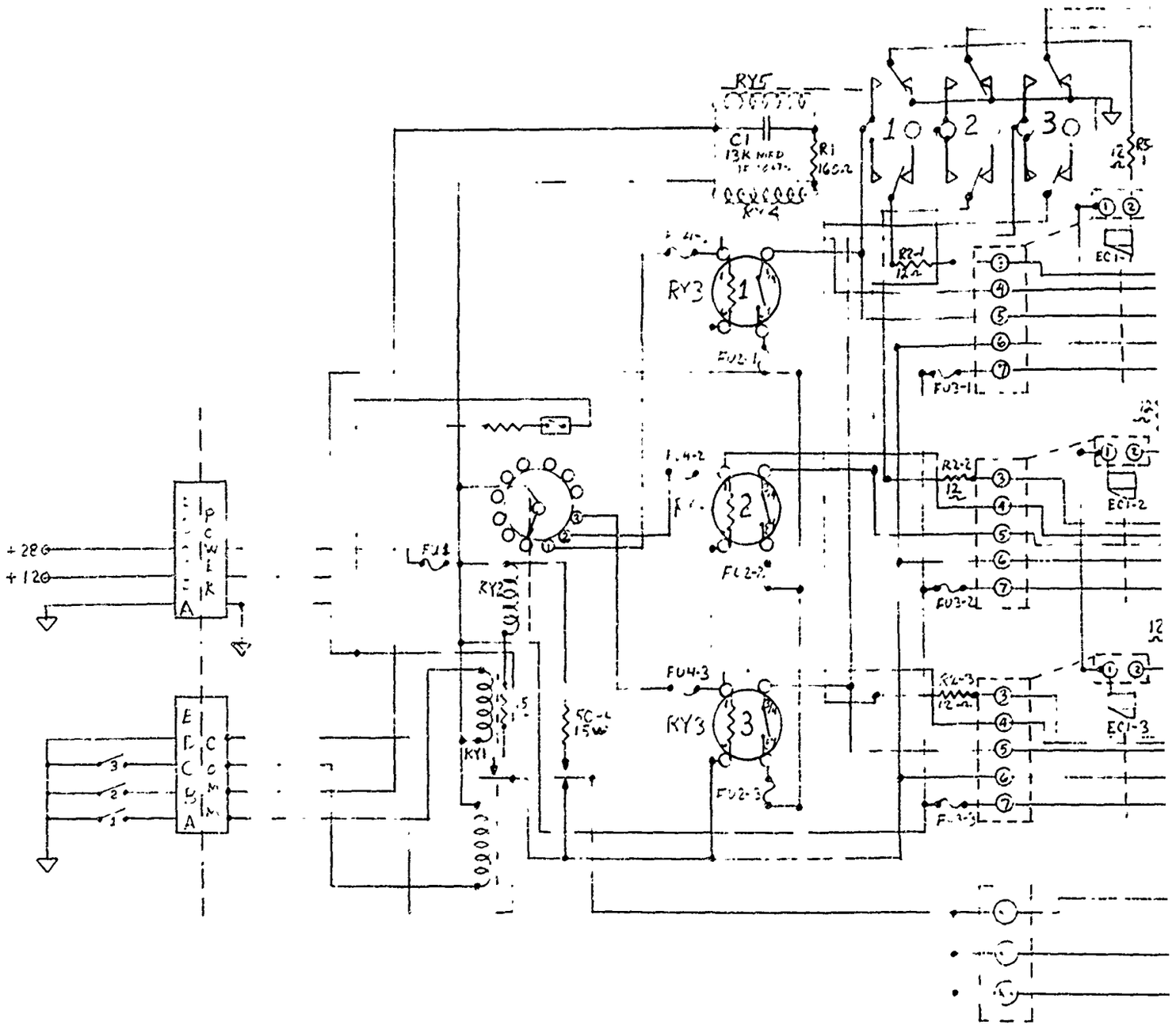

Figure 7. Schematic Diagram of Sonde Cutdown C

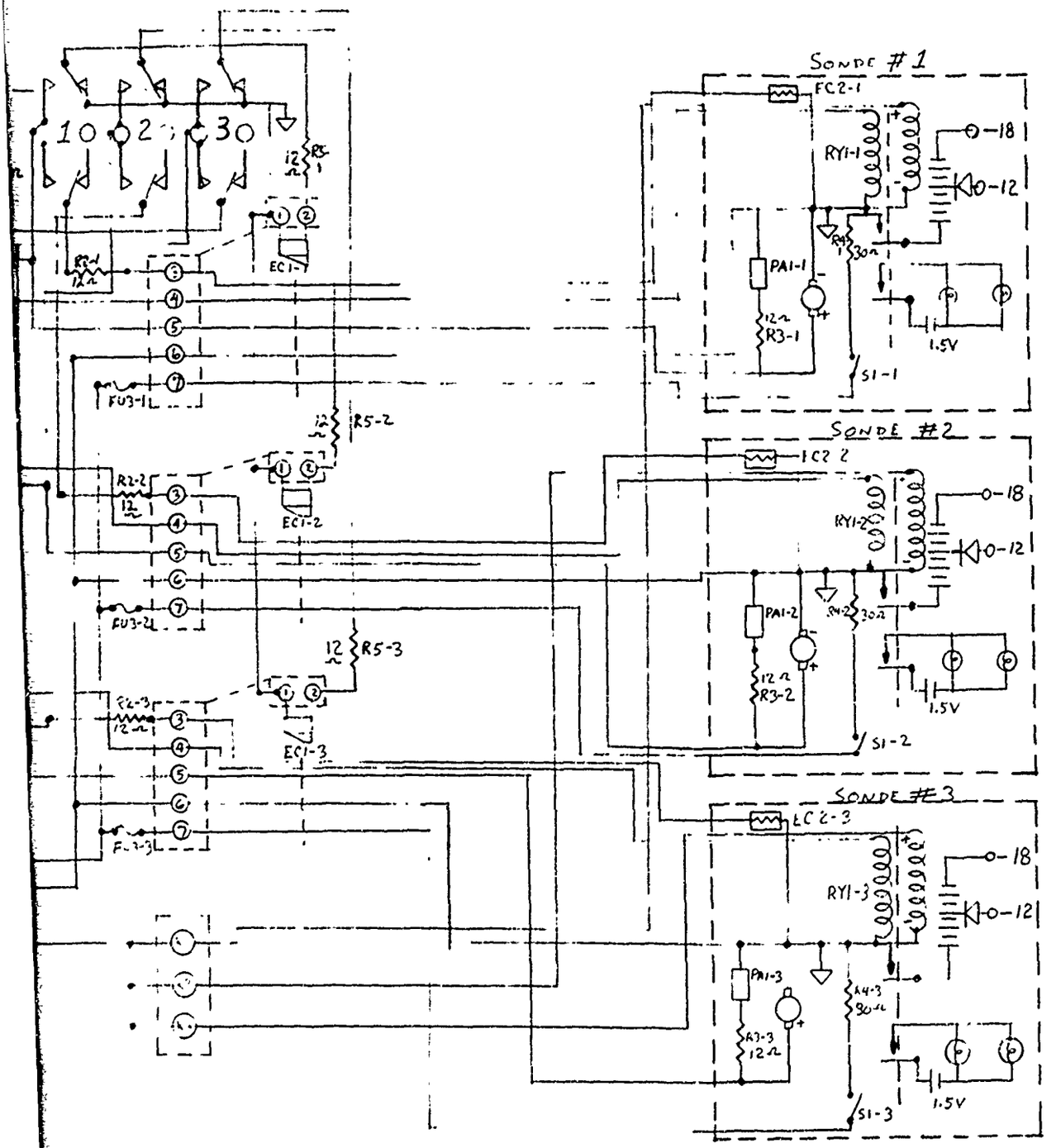

gram of Sonde Cutdown Circuit

SECTION V
WINDSONDE FLIGHT TEST PROGRAM

The flight tests of the Windsonde were conducted in two phases from Holloman AFB, New Mexico. The sondes were carried by balloon over the White Sands Missile Range and released at altitudes ranging from 30,000 to 35,000 feet. A typical flight sequence was as follows: The balloon was launched from an appropriate position such that all of the Windsondes could be dropped within range of the ground stations. A command signal from the ground started the sequence on the first sonde. This sequence allowed the air supply to reach the gyroscope's air bearing, started the transmitter, and started the spinup motor. After rotor speed was reached, the spinup motor withdrew, uncaging the gyroscope. The sonde was then released. The remaining sondes were released in succession, and the dispensers and associated electronics were parachuted to earth. Rawinsonde runs prior to and after the release of the sondes were made to aid in determining initial conditions and in the data analysis.

NOVEMBER 1967 FLIGHT TEST

The first test drops occured during the period 26 November through 2 December 1967. Three sondes were fabricated and taken to Holloman AFB, New Mexico, where final checks were made. These included supporting the gyroscope's rotor, testing each electronics, and assembling the sondes for the test drop. After two aborted balloon launch attempts, the sondes were dropped. (Details of the field test can be found in Reference 4).

A beacon was used on the flight to enable the ground stations to locate the balloon easily. This turned out to be a severe detriment rather than an aid because of failure of the squib to turn the beacon off. The first two sonde's signals were obliterated by the beacon and the only data obtained was an indication that both gyroscopes had spun up properly and intermittent rotor spin down rate. The third units' transmitter frequency was sufficiently different from that of the beacon that data were received over the altitude range of 32,200 to 23,000 feet. At this altitude the gyroscope's rotor lost bearing support, and no reliable information was obtained beyond that point.

NOVEMBER 1967 FLIGHT DATA ANALYSIS

For the first tests, the Windsonde data analysis was accomplished by feeding the tape-recorded tilt angle and roll position signals into a multichannel Honeywell Visicorder obtaining a continuous graphic record. Gyroscope pick-off angles were than scaled directly from the Visicorder chart. Roll position with respect to magnetic north was found by inspecting the roll sensor output

trace. The magnetic sensor was aligned in such a way that a negative peak on the roll sensor trace occurred when pickoff B pointed north, and a positive peak occurred when it pointed south. Zero crossings corresponded to east or west orientations. To ensure knowledge of the roll direction, deflectors in the launch fixture imparted a known initial roll to the sondes. Roll direction was chosen to be the same as the gyroscope rotor spin direction; as the rotor slowed down and transferred its angular momentum to the sonde body, it would tend to increase the roll rate slightly. An attempt was also made to maintain the roll rate throughout the flight by shaping the tail fins to give the effect of a small pitch angle. (The desired angle was calculated to be 0.15 degree.) Sonde data indicates, however, that an overall warping or misalignment of the tail fins overshadowed the effect of the pitch angle. The roll sensor trace shows that the roll rate decreased for the first few seconds, apparently stopping and then increasing again to approximately 1.5 rps. This behavior indicates that some aerodynamic property of the sonde (probably fin misalignment) caused it to reverse its roll direction during the flight.

Examing the gyroscope pickoff signals from sonde No. 3 on the Visicorder chart, a strong correlation was noted between the A and B pickoff outputs. If the tilt angle remains constant during a complete revolution, one would indeed expect the pickoff waveforms to be two sinusoids of equal amplitude and frequency. However, they should be 90 degrees out of phase with each other because the pickoff axes are perpendicular to one another. In this case the signals were nearly in phase with each other, which should occur only in the special case when the sonde is rocking in a plane bisecting the angle between the pickoffs. Faulty data transmission is the probable explanation here.

In laboratory tests, channel separation at the output of the ground station circuit had been excellent, but it appears that there was a severe crosstalk problem during the flight test. This probably resulted because we were modulating the RCA transmitters with the greatest deviation allowed by the receiver bandwidth in order to obtain maximum signal-to-noise ratio. However, if the receiver tuning was not precisely centered, the resulting distortion would lead to intermodulation and crosstalk between channels. In this case, it appears that serious distortion did take place to the extent that the subcarrier signal was masked by the direct modulation; in other words, both channels were dominated by signals from pickoff B.

Fortunately, when the sonde is rolling one gyroscope pickoff is sufficient to determine the tilt angle. The disadvantages are that fine structure may be lost, because the tilt angle must be averaged over some appreciable fraction of a revolution of the sonde, and the data readout cannot be readily automated.

Tilt angles used in the calculation of the wind profile for sonde number 3 were hand computed, using a graphical technique. Instantaneous pickoff B angles were scaled from the Visicorder chart at 90-degree roll position increments and plotted as vectors on polar coordinate paper. Magnitudes and direction of the resultants of each pair of consecutive vectors were then tabulated. These tabulated values represented the sonde's average orientation during the respective time increments and were fed into the computer for calculation of the wind profile. Any number of intersections could have been derived if more data points had been desired, but selecting 90-degree intervals simplified the task and afforded the best accuracy in determining intersection points.

Two rawinsonde runs were made to obtain wind data for comparison. The first run was released from the Jallen site at 0630 MST and reached 30,000 feet at about 1000 MST. The second run was launched from the Holloman site at 1240 MST and reached 30,000 feet at about 1320 MST. Since the usable Windsonde flight was released at 1204 MST, the available wind data is 2 hours before and 1-1/2 hours after our test flight. The radar that was to have tracked the sondes as they fell was unable to locate them, and as a result, the desired time-altitude-position information is not available.

The wind speed data are plotted in Figure 8 along with the two rawinsonde runs, while the wind direction is similarly shown in Figure 9. The Windsonde data agrees quite well with the rawinsonde data, even though the rawinsonde runs are separated both spatially and in time from the Windsonde drop. The sonde was clearly functioning and yielding wind information.

NOVEMBER POST-FLIGHT SYSTEM ANALYSIS

Aside from the failure of the beacon transmitter to cut off, difficulties with the data-transmission technique were minor. The major problems were the intermodulation between data channels and the required tracking of the balloon and sondes. With a balloon launch, the drop area cannot be fixed exactly, and the ground stations must be separated to ensure that one of them will be in range of the sondes. The narrow beam width of the GMD receivers required that the antenna be slewed. If signal strength is low, the chance of loss of data is increased.

All three gyroscope rotors appeared to be spinning down at the expected rate, but each one appeared to lose bearing support earlier than anticipated. A test program was run investigating the gas bottle filling process and the question of bearing failure at resonance. Using a programmed gas supply and an environmental chamber, simulated Windsonde tests were made. These tests indicated that the gas supply should have been adequate if the bottles had been filled properly. Since some of the gyroscopes have slightly larger flow

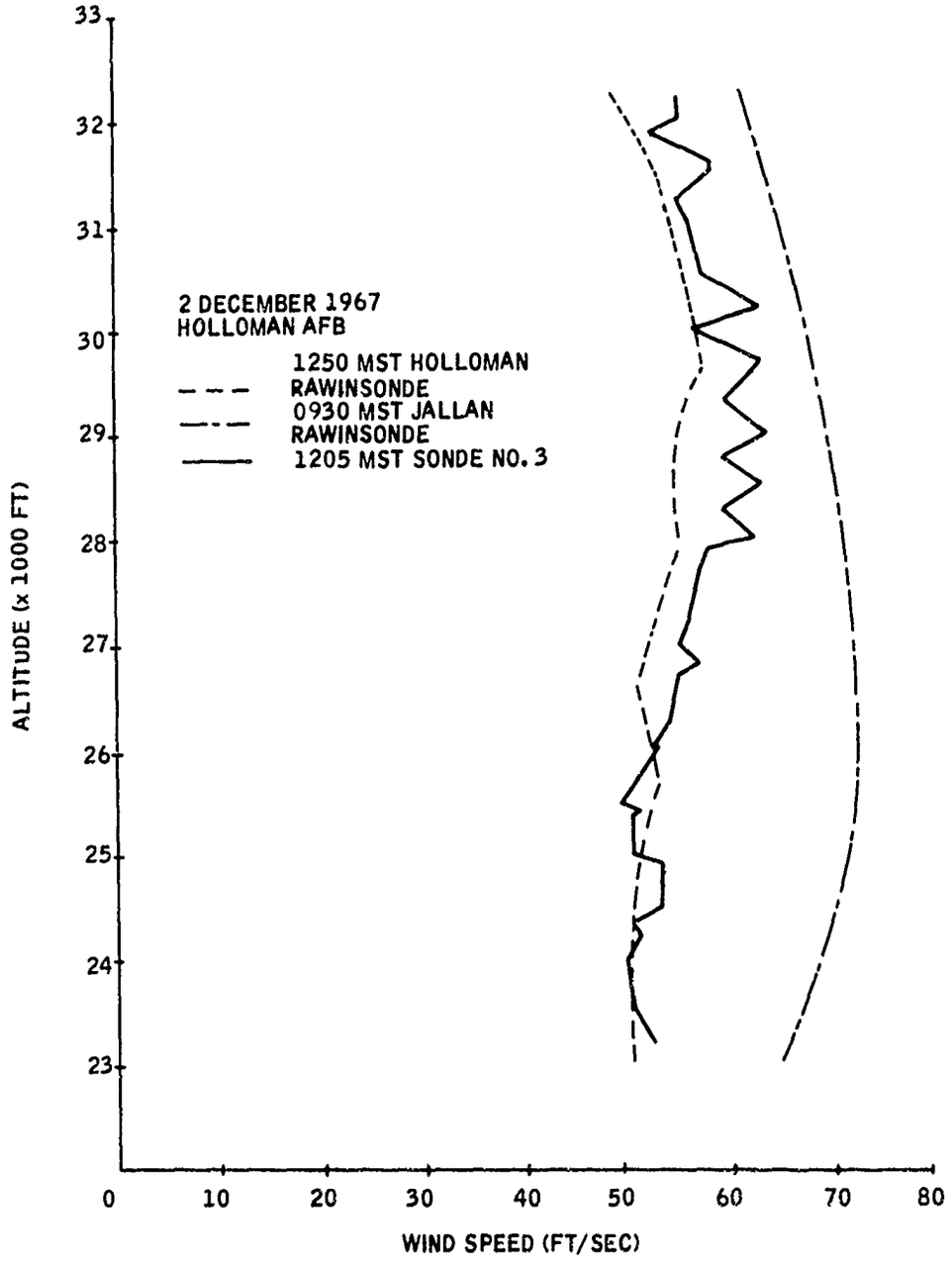

Figure 8. November Windsonde Test Result - Wind Speed

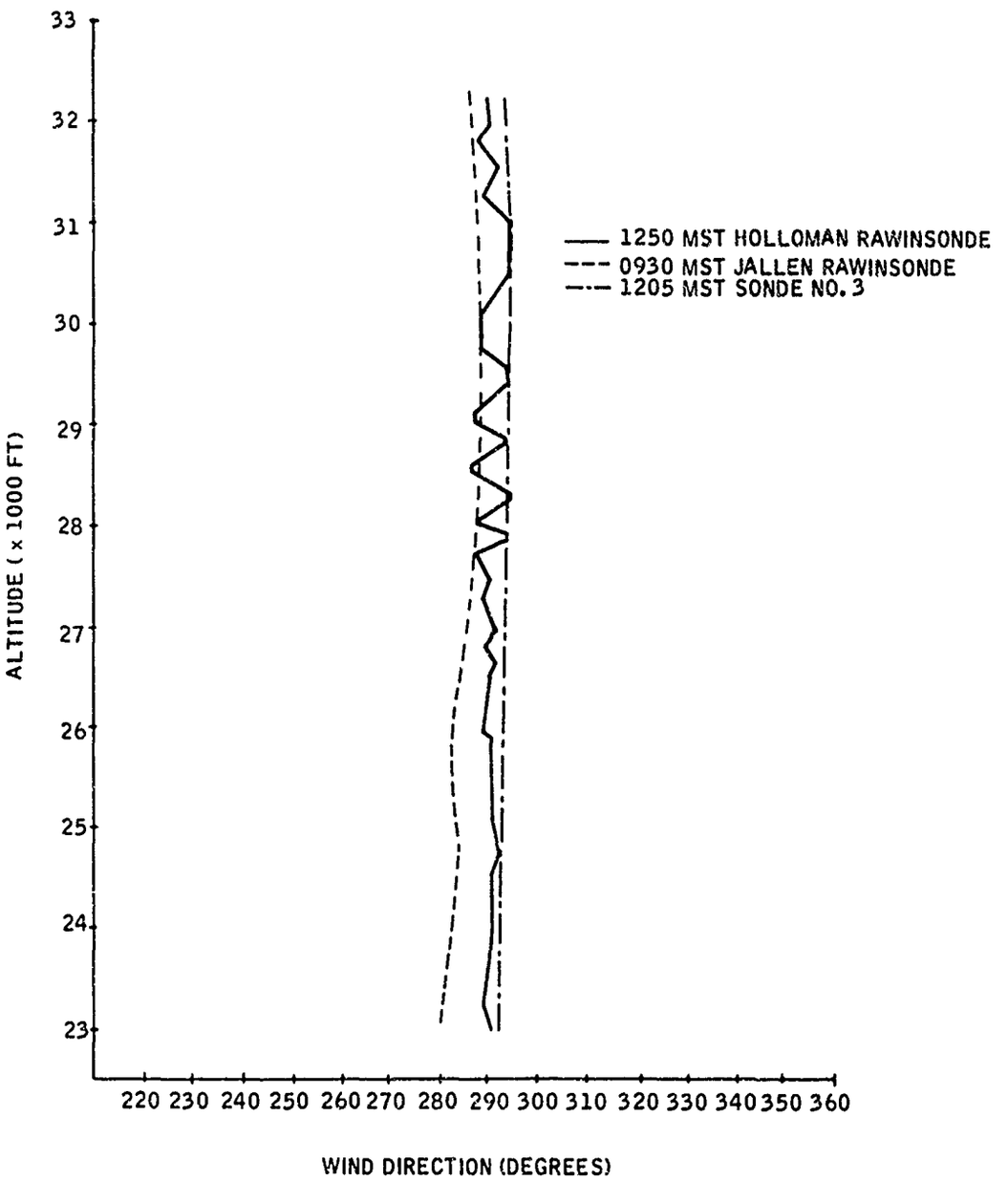

Figure 9. November Windsonde Test Result - Wind Direction

rates than others and since the gas bottles are structurally over-designed, it was decided that in the future each gas bottle would be filled to a minimum pressure of 4000 psi and would be cooled with Freon during the filling process.

Also included in the chamber tests were changing the rotor start speed and bearing support pressure. These tests showed no resonance problems in the expected operating range.

The results of these tests imply that the probable cause of the gyroscopes not fulfilling their mission was insufficient support gas. This was compensated for in the next units in two ways. The gas bottles were filled to 4000 psi, and the rotor spin up time was slightly shortened.

APRIL 1963 FLIGHT TEST

The second flight test program consisted of two flights with four sondes on each flight. The drop procedure was the same as on the earlier test, and basically the sondes were the same as those used on the first flight test. The major change reduced the gain in the pickoff circuits in an attempt to reduce the intermodulation between data channels. The tail surfaces were changed slightly as well. In order to maintain the roll direction and attempt to keep it uniform, ailerons were added to one pair of fins on each sonde.

The first test drop was scheduled for 29 April and the second for 1 May 1968. The sondes had been prepared as much as possible before going to Holloman AFB, New Mexico, to reduce the field time. The sondes were rechecked and prepared for launch while the equipment for the two ground stations was checked out.

The Holloman and Jallen GMD sites were again used as ground stations to receive Windsonde data. Although plans were to use one portable ground station for this drop test series, it was felt that adequate signal-to-noise ratios would not be obtained beyond a range of about 15 miles. This decision was reached after observing signals from a number of radiosondes launched at the Holloman site several days before the Windsonde tests. The uncertainty in predicting the balloon trajectory was great enough that a receiving range of at least 25 miles was desired.

A number of minor problems occurred, and these are discussed in Reference 5. The most serious thing was rough launches on both days; the canister containing the sondes was slammed against the launch truck as it started up, causing some problems in the sondes. Specifically sonde no. 2 on 29 April did not spin up; it is quite likely that the spinup motor was uncaged during the rough balloon launch. Similarly, sonde no. 1 on 1 May was not released. The tie cord was broken when the sonde was found in

the dispenser, and it must have occurred during the launch. The gyroscope in sonde no. 3 of 1 May started to spin up and then spun down. This could have been caused by a spin motor failure or by a partial uncaging of the motor at launch.

Noise and transmitter/electronics problems also caused a loss of data. The received signal from sonde no. 4 on 29 April was broken, and noise masked both pickoff A and the roll signal after 4 seconds. Sonde no. 4 on 1 May had a weak transmitter when tested just before launch. Some faint traces of signal were heard, but it is uncertain whether they came from the sonde.

Of the three remaining sondes, two had pickoff A only. Sonde no. 3 of 29 April had a very high noise level, and the roll information was good only from 13 to 47 seconds. Sonde no. 2 of 1 May had data from A and the roll signal from 2 to 40 seconds into the flight; it was then lost in the noise. Sonde no. 1 of 29 April had both channels present for 42 seconds of the flight. However, the roll signal was not usable until 18 seconds after the drop. Examination of the data showed that some intermodulation was again evident.

APRIL 1968 FLIGHT DATA ANALYSIS

Data from three of the sondes were reduced. Since sonde no. 1 of 29 April had shown signs of intermodulation, the data was reduced using the B pick-off only. Because the roll signal was not usable until 18 seconds into the drop, some assumptions concerning the fall position, sonde drift, initial wind, etc. had to be made. The result is shown in Figure 10.

Although the data agree within about 10 ft/sec with the rawinsonde run (and two rawinsonde runs may differ by more than that), and although assumptions had to be made about the start conditions, an attempt to improve the data was made. With the rough balloon launch it was possible that units other than those described above could have had their support cords cut. If this occurred the sonde could be uncaged while not hanging vertically, and a bias angle would be added to the data.

To determine what tilt angles should have occurred, the wind profile and sonde characteristics can be taken and the angle determined analytically. Since the only wind information available was the 0900 Jallen rawinsonde run, this information was used. The result indicated that a 0.75-degree angle should be added to the data. This reduced the deviation between the Windsonde and rawinsonde data. However, with all the uncertainties concerning the initial conditions, the validity of this correction is uncertain.

Although the data from sonde no. 1 of 29 April had showed channel intermodulation and sonde no. 3 of that same day had only channel A information which would probably be similarly affected, the data was reduced. Since there was no data for the first 13 seconds, start condition assumptions had to be made. The reduced wind data tends to remain too high, and no easy correction can be made that significantly improves it. The likely problem is the intermodulation by the noise of channel B.

Sonde no. 2 of 1 May appeared to have good data for 40 seconds of the flight. However, a curve of rotor speed vs time showed a sharp slope change at 15 seconds, indicating that the rotor had been touched by the bearing or a piece of foreign matter. A correction was again required since the actual tilt angles and computed tilt angles disagreed. After adding the correction, the data agreed quite well with the rawinsonde data until the point of rotor speed slope change, where they diverge rapidly.

APRIL POST-FLIGHT SYSTEM ANALYSIS

It appears that the data transmission was a major problem. As previously mentioned, the signals were very noisy and required additional filtering to make them usable. Pickoff B signals, which directly modulate the transmitter, were in some cases not transmitted because of some undetermined component failure. This left only the pickoff A signal which, along with the magnetic sensor output, is present on the subcarrier signal. A considerable amount of interaction between the pickoff and roll signals is possible when the signal-to-noise ratio is poor, as it was on the drops. When the noise level is high, the angle-decoding circuit becomes sensitive to the amplitude of the pickoff signal, and this amplitude can be affected by roll in two ways. The received radio-frequency signal fluctuates as the sonde rolls because of asymmetry in the antenna pattern. If there is not enough incoming signal to produce limiting in the FM receiver, the detected pickoff signal level is seriously affected by changes in the carrier amplitude. Also, since the overall bandpass of the system is not completely flat, the subcarrier frequency swing produced by the magnetic aspect sensor also induces some change in detected subcarrier amplitude, which again reflects in the pickoff A signal. Even though the degree of interaction is small, it seriously affects the derived wind profile because the resulting in-phase errors in the tilt and roll angle readouts lead to a cumulative wind-velocity error when integrated. Other random signal fluctuations resulting from multipath transmission and "jerky" antenna tracking contributed to the noise problems.

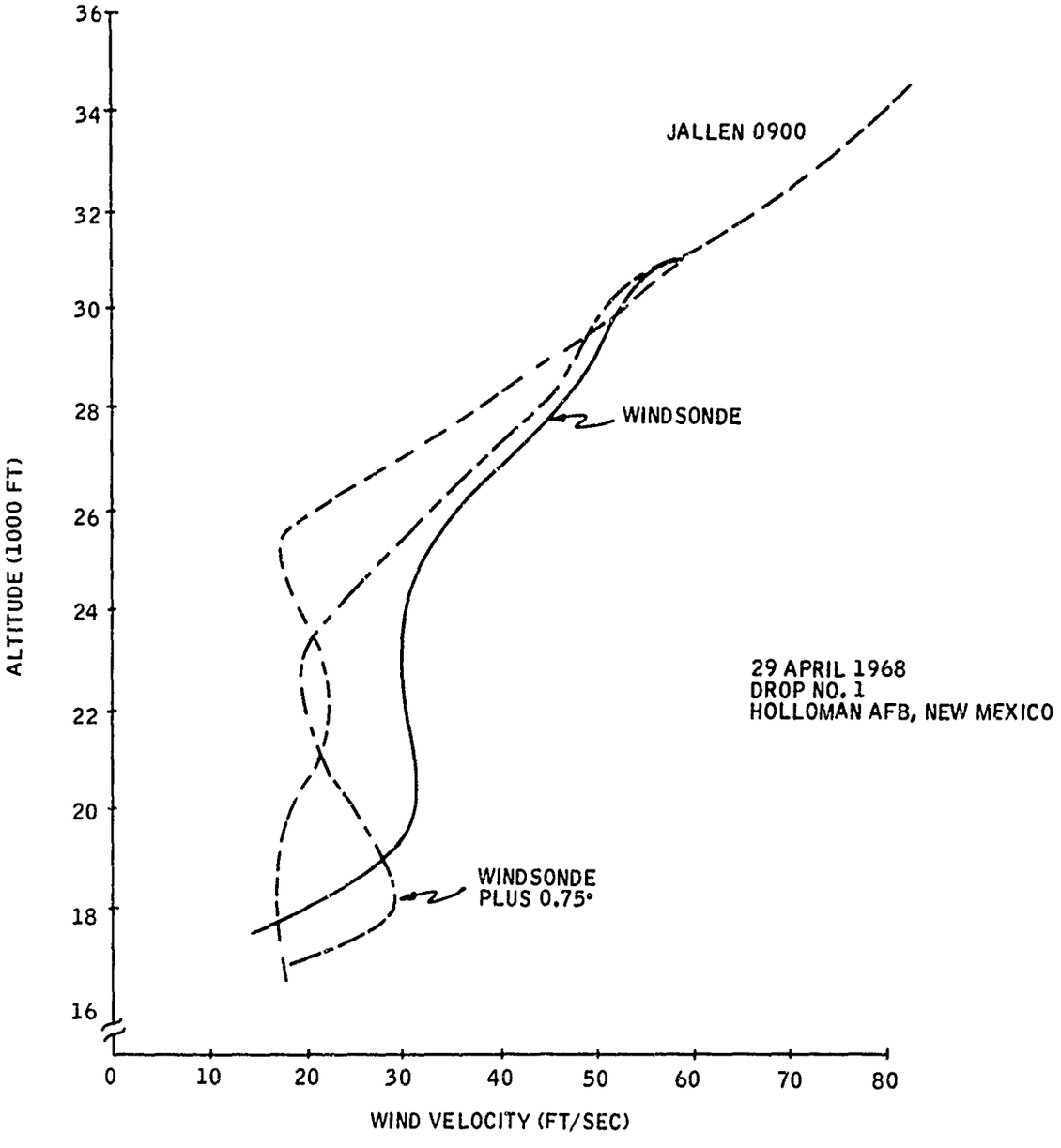

Figure 10. April Windsonde Flight

SECTION VI
CONCLUSIONS

A number of problems ranging from rough balloon launches to data transmission difficulties occurred during the balloon flight test program. The amount of data received was limited. However, the results do indicate that the Windsonde does respond to wind shears as it falls. It is difficult to determine response time and accuracy of the system with the data obtained and the supporting information supplied. The radar was unable to track any of the sondes. As a result we could not correlate indicated sonde motions with actual events and estimate errors. On the first flight test the rawinsonde runs yielding wind information that were available for comparison differed both spatially and in time from the Windsonde and one another. They also showed a 12-ft/sec difference between the two rawinsonde profiles.

The rawinsonde data is smoothed over 2000-foot intervals, so it is difficult to correlate response times when comparing wind data. However, it is evident that the Windsonde will respond more quickly.

During the first flight test, the gyroscope gas supply was found to be deficient. This was changed and proved adequate during the second flight test. Intermodulation of data channels also proved to be a problem on the first tests. The attempt to improve this situation was not successful as there was still some intermodulation during the second tests. It is apparent that future sondes will require more complete channel separation, such as by using a voltage-controlled oscillator to handle one channel.

There is little question that, with improved electronics to ensure data separation, the Windsonde is capable of responding to wind shear and of determining the amount of the shear. By integrating, a vertical profile of the wind can be obtained. The next test phase of ejecting sondes from an aircraft should be undertaken.

REFERENCES

1. Honeywell Proposal 6D-G-26, "Air-Launched Windsonde", in response to USAF Cambridge Research Laboratories RFQ No. CRL63175, 22 March 1965.

2. Honeywell Document 12042-QR4, Fourth Quarterly Progress Report on Contract AF19(628)-6082, 15 June 1967

3. Honeywell Document 12042-QR5, Fifth Quarterly Progress Report on Contract AF19(628)-6082, 15 September 1967

4. Honeywell Document 12042-QR6, Sixth Quarterly Progress Report on Contract AF19(628)-6082, 15 December 1967

5. Honeywell Document 12042-QR8, Eighth Quarterly Progress Report on Contract AF19(628)-6082, 15 June 1968.

Unclassified

Security Classification

DOCUMENT CONTROL DATA - R & D

(Security classification of title, body of abstract and indexing annotation must be entered when the overall report is classified)

1. ORIGINATING ACTIVITY (Corporate author)	2a. REPORT SECURITY CLASSIFICATION
Honeywell Inc. Systems and Research Division, Research Dept. St. Paul, Minnesota 55113	Unclassified
	2b. GROUP NA

3. REPORT TITLE

AIR-LAUNCHED WINDSONDE

4. DESCRIPTIVE NOTES (Type of report and inclusive dates)

Scientific Interim

5. AUTHOR(S) (First name, middle initial, last name)

Stephen F. Rohrbough
Lyle E. Koehler

6. REPORT DATE	7a. TOTAL NO. OF PAGES	7b. NO OF REFS
July 1969	54	5

8a. CONTRACT OR GRANT NO.	9a. ORIGINATOR'S REPORT NUMBER(S)
AF19(628)-6082 b. Project, Task, Work Unit Nos. 6670-02-01 c. DoD Element: 6240539F d. DoD Subelement: 681000	12042-SR1 Scientific Report No. 1
	9b. OTHER REPORT NO(S) (Any other numbers that may be assigned this report) AFCRL-69-0397

10. DISTRIBUTION STATEMENT

1-Distribution of this document is unlimited. It may be released to the Clearinghouse, Department of Commerce, for sale to the general public.

11. SUPPLEMENTARY NOTES	12. SPONSORING MILITARY ACTIVITY
TECH, OTHER	Air Force Cambridge Research Laboratories (CRE) L. G. Hanscom Field Bedford, Massachusetts 01730

13. ABSTRACT

The design, development, and first phase of the testing of a wind measuring instrument are described. The device was required to obtain a vertical profile of winds to sea level after being released from an aircraft at 30,000 feet. An arrow-shaped, low wind-drift sonde was selected that used an air-bearing gyroscope and magnetic field sensor to measure data that yielded wind shear. This information was then integrated to obtain wind velocity. The results of the balloon-launched phase of the field tests indicated that the sonde does respond to the wind and that the second test phase involving aircraft deployment of the sondes should be undertaken.

DD FORM 1 NOV 68 1473 REPLACES DD FORM 1473, 1 JAN 64, WHICH IS OBSOLETE FOR ARMY USE.

Unclassified

Security Classification

14 KEY WORDS	LINK A		LINK B		LINK C	
	ROLE	WT	ROLE	WT	ROLE	WT
Windsonde						
Wind						
Wind Shear						
Acceleration						
Gyroscope						
Dropsonde						